

Supplementary material 1

Maciej Orkisz, Alfredo Morales Pinzón, Jean-Christophe Richard,
Claude Guérin, Leslie E. Solórzano Vargas,
Daniela Sicaru, Camila García Hernández,
Margarita M. Gómez Ballén, Bruno Neyran,
Eduardo E. Dávila Serrano, Marcela Hernández Hoyos

June 14, 2019

Curves representing regional-recruitment values vs. PEEP in example regions (Figure S1) show that the values obtained using warped boxes were consistently positive and predominantly decreasing when PEEP increased, while they were somewhat chaotic when the shape changes of the boxes were neglected.

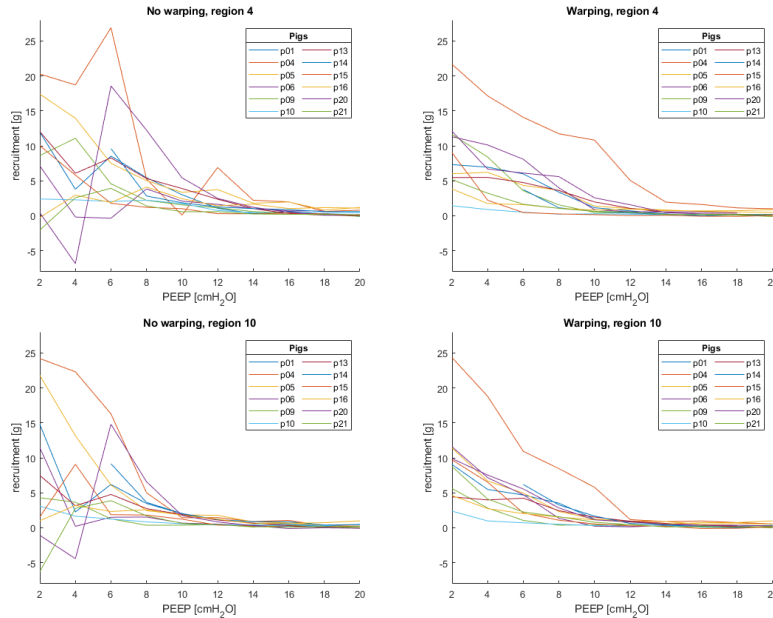


Figure S1: Regional-recruitment values, calculated in big boxes (Experiment 2) as a function of PEEP: (*left*) approach **c**, (*right*) approach **d**. The selected example regions, 4 and 10, were located at mid-height in the posterior part of the right and left lung, respectively.

Variance ratios F obtained in regional-recruitment quantification using big boxes (Table S1) also demonstrate that the results obtained in warped boxes were systematically better than without warping.

Table S1: Variance ratios F obtained in big boxes (Experiment 2) with approaches **c** and **d** for factors PEEP and pig. Bold characters highlight the better result in each pair (**c** vs. **d**).

Box #	Box location			factor PEEP		factor pig	
				c	d	c	d
11	top	posterior	left	4.4	10.0	2.2	2.3
10	middle	posterior	left	4.5	25.7	2.4	6.4
9	bottom	posterior	left	8.4	30.6	2.2	8.5
8	top	anterior	left	1.6	4.1	4.6	12.2
7	middle	anterior	left	4.3	15.4	3.2	5.5
6	bottom	anterior	left	7.9	12.8	3.3	5.9
5	top	posterior	right	1.9	8.8	3.2	4.7
4	middle	posterior	right	6.5	24.0	3.1	10.2
3	bottom	posterior	right	3.0	29.0	1.7	16.0
2	top	anterior	right	10.4	13.3	8.5	11.4
1	middle	anterior	right	5.5	11.5	4.3	6.6
0	bottom	anterior	right	8.3	12.7	3.4	5.3

Figures S2 and S3 respectively display regional- and local-recruitment maps with decreasing box sizes, overlaid onto the original image in example axial, coronal, and sagittal cuts. They show that increased localization amplifies sensitivity to registration errors (see unlikely derecruitment displayed in blue color) illustrated by Figure S3 bottom: Before registration (third row), big arrows show the displacement of the diaphragm (sagittal view), and density differences mainly due to recruitment, because the non-aerated region shrunk at end-inhale (axial view). After registration (last row), these arrows respectively show good alignment of the diaphragm, and erroneous alignment of the non-aerated-region boundary. Smaller arrows indicate examples of misaligned artery and airway walls: the registration algorithm uselessly attempted to align the boundary of the shrunken non-aerated-region, while “dragging” anatomical structures.

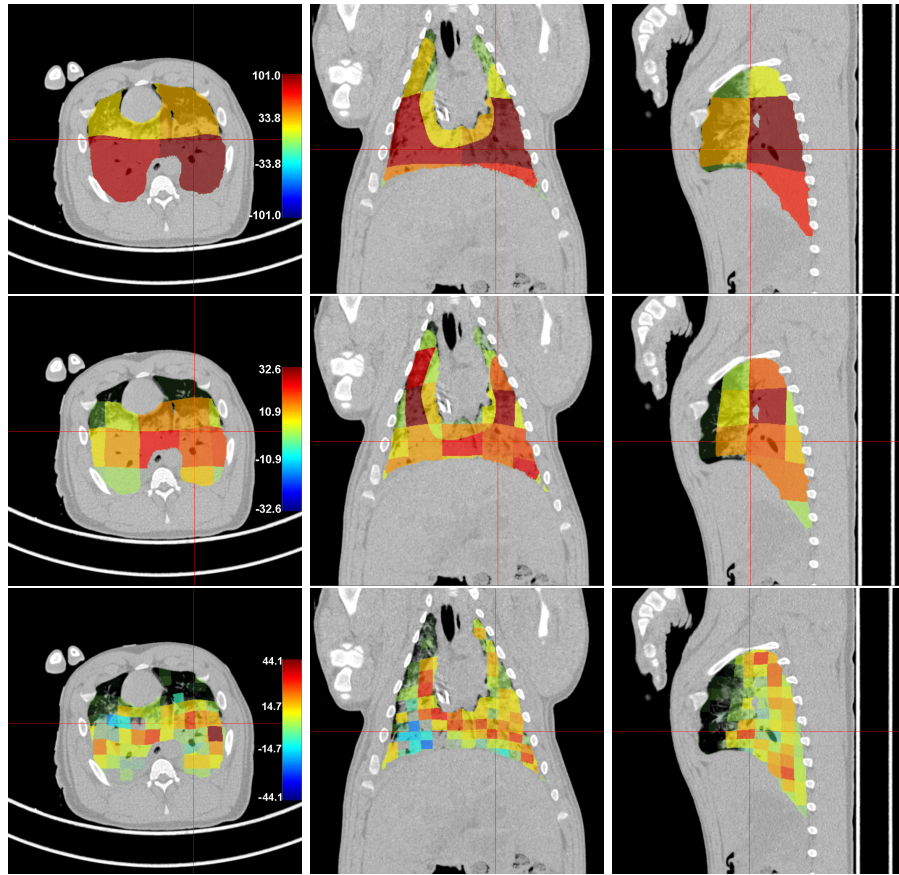


Figure S2: Orthogonal cuts through regional-recruitment maps overlaid onto the corresponding original image and calculated in big, medium and small boxes, respectively. In the second and third rows, the green color representing zero recruitment was made more translucent to improve legibility.

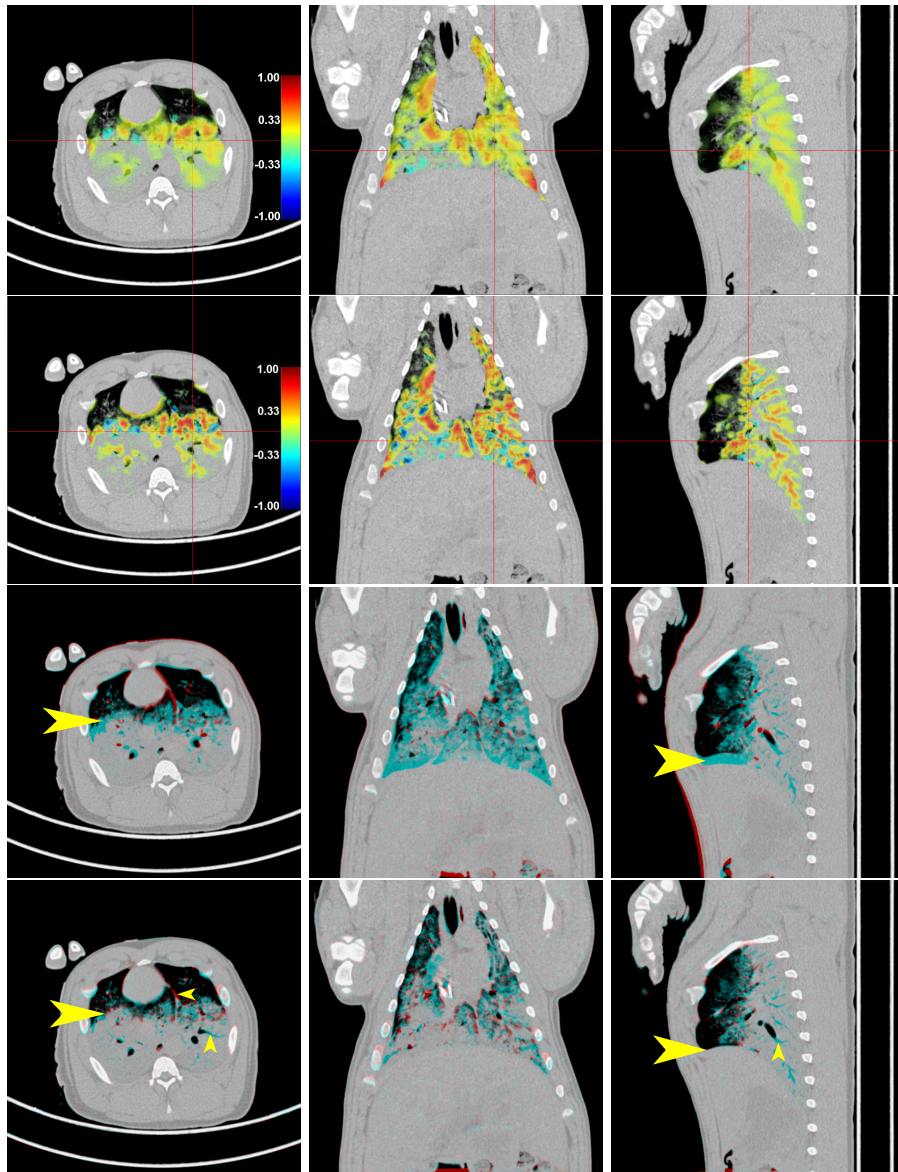


Figure S3: Local recruitment and registration results. Orthogonal cuts through local-recruitment maps overlaid onto the corresponding original image and calculated with box sizes of 10 (first row) and 5 mm (second row). The green color representing zero recruitment was made transparent to improve legibility. Corresponding end-inhale and end-exhale images superimposed before (third row) and after registration (fourth row). Colors highlight regions where densities do not coincide. Big arrows indicate boundaries before and after alignment. Smaller arrows show examples of misaligned artery and airway walls.

Figure S4 displays a 3D representation of example axial, coronal, and sagittal cuts through local-recruitment maps, overlaid onto the original end-exhale images acquired at varying PEEP values. Sub-figures correspond to frames of a supplementary video¹. It can be seen that the posterior non-aerated region shrinks as PEEP increases. Intratidal recruitment decreases as PEEP increases, although its density is heterogeneously distributed throughout the lungs.

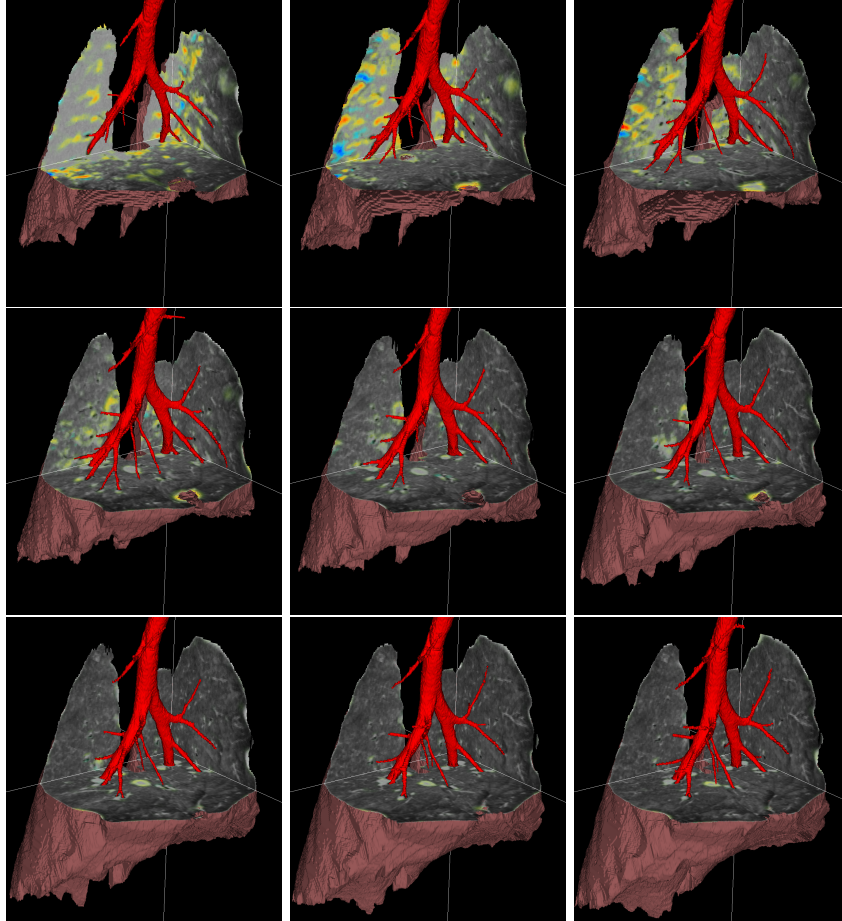


Figure S4: Three-dimensional representation of orthogonal cuts through a local-recruitment map overlaid onto the corresponding original image acquired at PEEP values ranging from 2 to 18 cm H₂O.

¹https://www.creatis.insa-lyon.fr/~orkisz/pig20_changing_PEEP.mp4

In Figure S5 each point represents the sum of local-recruitment values calculated within the entire segmented lungs of one pig at one pressure vs. the global-recruitment value calculated in the same pig at the same pressure. Differences between the results obtained with box sizes of 5 and 10 mm (left and right columns, respectively) are hardly perceptible. The integrated local values were consistent with the global values, but the linear regressions were hampered (top row) by four points corresponding to the lowest PEEP values in pig 4, where interactive delineation of the lung, as well as automatic image registration, were particularly challenging. The bottom row shows the improvement of the regressions after removing these outliers.

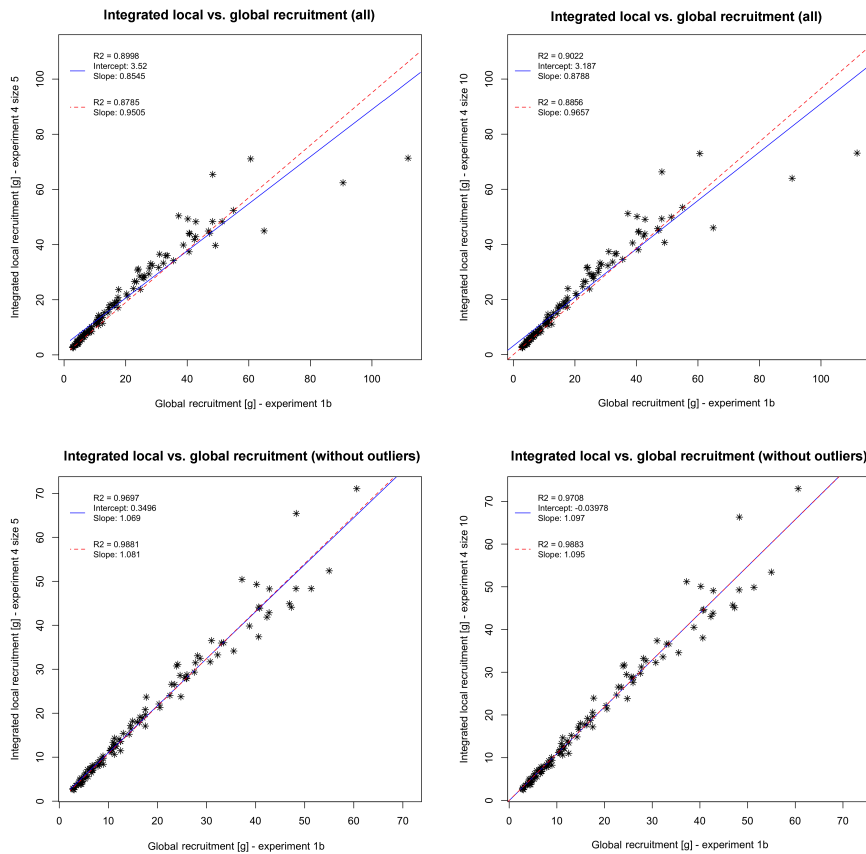


Figure S5: Linear regressions between the local-recruitment values integrated over the whole segmented lungs and the global-recruitment values, for local values calculated with box size of 5 mm (*left*) and 10 mm (*right*), for all pigs and all PEEP values (*top*), and excluding the low-PEEP outliers from pig 4 (*bottom*). Dashed lines represent regressions made with intercept forced to zero.

In Figure S6 each point represents the sum of local-recruitment values over one region (big box) in one pig vs. the regional-recruitment value (Experiment 2) calculated in the same region of the same pig at the same pressure. The right column clearly shows that the integrated local values were consistent with the regional values calculated within warped regions, except a few points corresponding to the lowest PEEP values in pig 4 excluded in the bottom row. On the contrary, the results obtained within regions without warping (left column) were not consistent at all, which once again demonstrates the importance of taking into account the tissue motion.

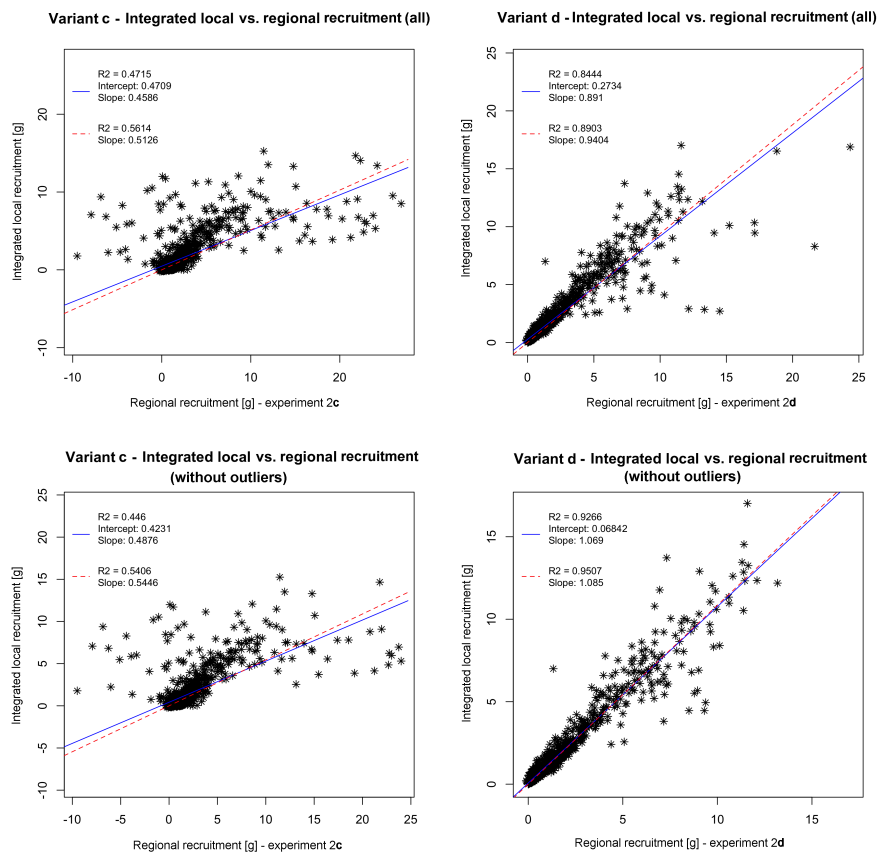


Figure S6: Linear regressions between the regional-recruitment values in big boxes and the local-recruitment values integrated over the same regions, for regional values calculated with the approach **c** (left) and **d** (right), for all regions and all pigs (top), and excluding the low-PEEP outliers from pig 4 (bottom).

The results obtained in Experiment 3 with medium-size boxes displayed similar trends (Fig. S7). After the exclusion of the low-PEEP outliers from pig 4 (right), the slope of the linear regression was close to one, and the dispersion was reasonably small ($R^2 = 0.81$).

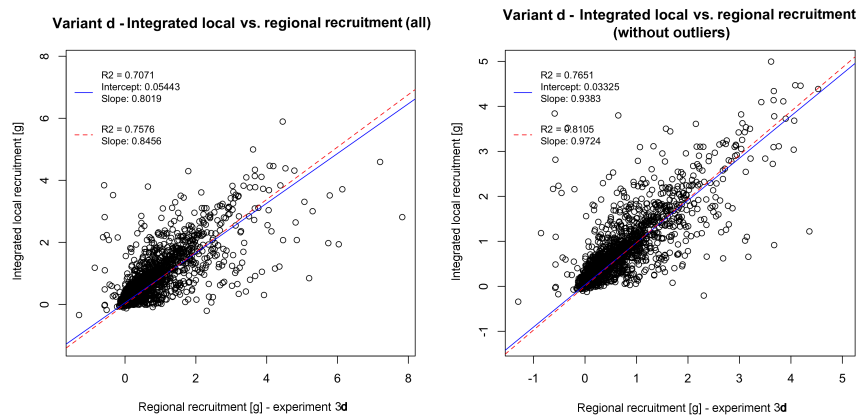


Figure S7: Linear regressions between the regional-recruitment values in medium-size boxes and the local-recruitment values integrated over the same regions, for regional values calculated with the approach **d** in all regions and all pigs (*left*), and excluding the low-PEEP outliers from pig 4 (*right*).